Examination of the microstructure of hydroxyapatiteQ1 with respect to pH and calcination temperature for varying concentrations of zinc

P.Venkat Reddy ¹, M.Navaneetha ²,
Associate Professor ^{1,2,}
Department of Mathematics,
BRILLIANT GRAMMAR SCHOOL EDUCATIONAL SOCIETY'S GROUP OF INSTITUTIONSINTEGRATED CAMPUS
Abdullapurmet (V), Abdullapurmet (M), R.R Dt. Hyderabad.

Abstract

This Q4 project set out to describe the impact of solution pH and calcination temperature on the structure, chemical content, and particle/crystallite size of hydroxyapatite (Hap). Powders of nonstoichiometric Hap (nap) with a zinc percentage of 4 at.% were produced using a solution-precipitation technique. X-ray diffraction (XRD), energy dispersive spectroscopy (EDS), Fourier transform infrared spectroscopy (FTIR), and scanning electron microscopy (SEM) were used to characterise the impact of pH (values: 9 and 10.5) and two calcination temperatures (550 and 1000C) on chemical composition, molecule internal bonds, particle, and crystallite size of the synthesised powders. Incorporating zinc cations into the atomic structure of Hap led to the formation of a low crystalline single phase of nap. As the pH was lowered to 10.5, powders with finer particle and crystallite sizes began to develop. Decomposition of zinc-doped nap into the biodegradationregulating -tricalcium-phosphate and triazincalcium-phosphate phases was also seen at calcination temperatures up to 1000 degrees Celsius..

Introduction

The inorganic material hydroxyapatite (Hap) found mostly in bone and teeth has found applications in several biological disciplines. The network of the Hap structure is very amenable to replacements, allowing for ions other than calcium or phosphate to be inserted into the Hap structure in lieu of those two ions [1,2]. Lattice parameters, crystallinity, symmetry. thermal stability. morphology. solubility, and physical, chemical, and biological properties are only some of the things that might alter because of a substitution group [3]. One of the most consequential cations that may be integrated into the Ca sites of the atomic structure of Hap is the zinc cation (Zn). Research shows that this cation is highly osteoconductive and may promote

bone growth [4-7]. This has led to the development of a biphasic calcium phosphate (BCP) bio ceramic with both Hap and TCP phases, which allows for regulation of the biodegradation rate. For the most part, the chemical formula for a nap in biological systems looks like Eq. (1):

$$Ca_{10-x}(HPO_4)_x(PO_4)_{6-x}(OH)_{2-x}$$

Apatite's may be biologically precipitated using -TCP, which is more soluble than nap despite having a nearly same chemical makeup but a distinct crystalline structure [3]. Recent studies [8– 10] have focused on the intriguing topic of Zn incorporation into the Hap structure. Zn2+reduces the crystallinity of the Hap structure by encouraging the synthesis of TCP [11] and is thus known to have an inhibitory influence on Hap formation. The chemical composition and particle size of the precipitated powders are affected by the pH of the solution, the concentration of the mixing reagents, the temperature of preparation, and the temperature of calcination [12]. Hydrothermal, solgel, spray-pyrolysis, and wet chemical procedures are all viable options for synthesising calcium phosphate powders [13,14]. The wet chemical precipitation approach was used to manufacture zinc-doped Hap nano powders in this research. The new contribution of this work is the study of the effect of zinc cations on the atomic structure of Hap as a function of solution pH and calcination temperature. TG-DTA, EDS, X-ray diffraction, FT-IR, and scanning electron microscopy were used to investigate the products' atomic structure and

Materials and methods

Separately, we made aqueous solutions of phosphorous (0.06 mol) and calcium (0.1 mol) salts by dissolving, respectively, 0.1 mol hydrate calcium acetate (Ca (CH3COO)2H2O, Merck, 99% pure, Art No. 1.09325.0500) and 0.06 mol diammonium hydrogen phosphate ((NH4)2HPO4, Merck, 99% pure, Art No. 1.01207. The two solutions were combined by slowly adding the

second one while being stirred vigorously at 45 degrees Celsius. The final solution's pH was adjusted with 0.1 M ammonia to a range from 9 to 10.5. Ten hours were spent drying the granules that had precipitated out. Using the same steps as previously, zinc acetate dihydrate (Zn (CH3COO)22H2O, Merck, very pure, Art No. 1.08802.0250) was added to hydrate calcium acetate solution to produce Zn-incorporated Hap powders. In all the tests, the molar ratio of (Ca + Zn)/P remained at 1.67. The percentage of zinc to zinc and calcium was settled on at 4 at. %Zinc. Lastly, the powders were calcined at 550 and 1000 C to examine how zinc cation affected the resulting calcium phosphate's chemical composition and particle size. Table 1 contains the relevant example codes for your convenience.

Characterizations

Appropriate calcination temperatures determined with the use of thermogravimetricdifferential thermal analysis (STA equipment). Phase analysis of produced powders was performed using X-ray diffraction with a scanning range of 2 = 10-80(Cok1 = 1.78901 A, Nifiltered); Philips PW2273 diffractometer. Standard JCPDS data were used to examine the phases formed during precipitation and after calcination. For this study, we used an **FTIR** spectrophotometer, model number Vector 33-Bruke, calibrated to the ASTM 1252 standard, to look at the structural changes of the molecular bands in the material. With the use of a scanning electron microscope (VEGA-TESCAN) coupled with an EDS analyser, the morphology and chemical content of the powders were analysed. Using an image analyser, we dropped a drop of a solution of manufactured powders onto a glass slide and sputter-coated it with 10 nm of gold to estimate the particle size. Using Sherrer's equation [15], the crystallite size of the produced powders was calculated from the X-ray line broadening.

$D = 0.9\lambda/\beta\cos\theta$

where D is the size of the crystal, is the radiation wavelength, is the Bragg's angle, and is the full width at half maximum.

Results and discussion

Appropriate calcination temperatures were determined using TG-DTA analyses. Figure 1 displays the samples' TG-DTA profiles. Desorption of water from the surface of nap causes a loss of mass below 150 °C and is responsible for the endothermic peak at these temperatures. Reduction in volume due to loss of water and condensation of

Table 1

Conditions of powder preparation and their codes.

Zn/(Ca+Zn)	pH 9		pH 10.5	
	25°C	25 °C	550°C	1000°C
0	0ZH1	OZH2	0ZH2-550	0ZH2-1000
4	4ZH1	4ZH2	4ZH2-550	4ZH2-1000

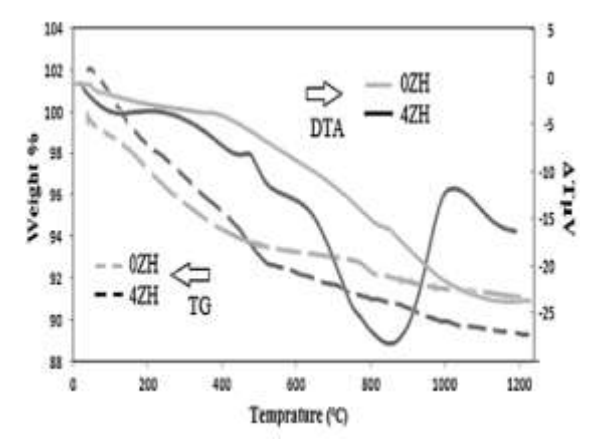


Fig. 1. TG-DTA profiles of the products. 0 at. % zinc fraction (grey lines) and 4 at.% zinc fraction (black lines).

At temperatures between 150 and 600 °C [16], the HPO42group might form, and the lattice water could vaporise. Low-range dehydration and condensation of the HPO42-group in 4ZH1 powders were seen as a faint peak about 480 °C in the DTA curve and a corresponding weight loss in the TGA graph. As a result, it is reasonable to assume that Zn2+do not affect the atomic structure of Hap below 600C. At temperatures over 600 °C, the 0ZH1 sample showed no notable peaks, suggesting that no new phase was formed or decomposed. Decomposition of the nap and generation of the tri calcium phosphate (Ca3(PO4)2) and/or tri zinc phosphate (Zn3(PO4)2) were indicated by the presence of a broad endothermic peak at 700-950C in the sample containing 4 at.% zinc fraction. The peak's broad temperature range indicates breakdown occurs across a broad temperature range. Hence, 550 and were 1000C candidate temperatures calcinations in order to clarify the Q5 impact of calcinations on the atomic structure of free zinc and zinc doped Hap.

Chemical composition and phases

Fig. 2 displays the energy dispersive spectroscopy (EDS) spectra of pH 9 nap powders with and without zinc incorporation. Their spectra have overlapped, except for the highlighted region on the right side of Fig. 2 where the energies are 0.8–1.2 keV. To counteract the effects of Zn-loss Laps of X-ray energy, zinc is often doped into nap. That's why you'll find both calcium and zinc here.

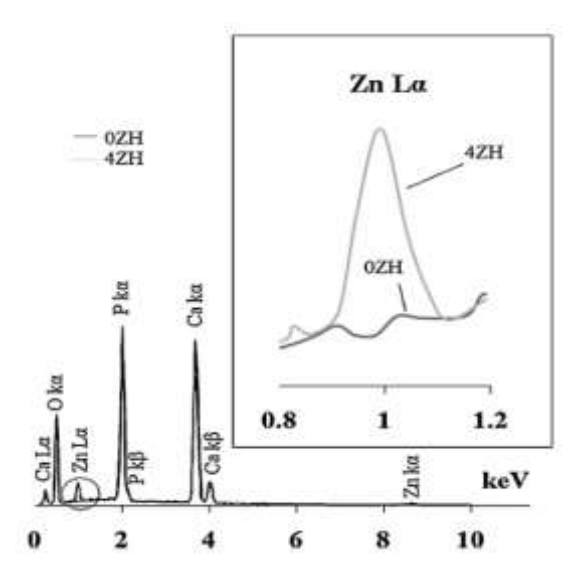


Fig. 2. The EDS spectra of entire and zinc incorporated nap.

And both samples were found to contain phosphorus. As a rough approximation, the molar ratio of (Ca + Zn)/P in the synthesised powders was 1.64 for the zinc-free samples and 1.58 for the zincincorporated ones. The powders produced at pH 10.5, although at different temperatures, showed identical results in terms of EDS spectra and (Ca + Zn)/P molar ratios. In Fig. 3, we see a graph of the X-ray patterns of Hap powders with and without zinc, produced at various pH levels and calcined at various temperatures. Based on their X-ray diffraction patterns, Fig. 3(a) and (e) reveal that both 0ZH1 and 4ZH1 are composed of a single crystalline nap phase, with the former containing free zinc and the latter including calcium-phosphate granules. As can be observed in Fig. 3(a) and (b), the crystallinity of Hap powders was reduced after being doped with 4 at.% Zn2+ (e). The crystallinity and scheme of the XRD pattern of synthesised 0ZH powders exhibited no discernible change while the pH was increased from 9 to 10.5. Calcination of the synthesised powders at 550°C not only did not result in the formation of any new phases, but it also did not result in any significant changes in the crystallinity of either type of powders, except for a slight shift in the peak with respect to the (2 1 1) plane in the 4ZH sample. During 550°C calcinations, the (2 1 1) plane is shifted to a lower angle due to the difference in ionic radii between Zn2+(0.074 nm) and Ca2+ (0.099 nm), as shown by Q6. TG-DTA analysis, which predicts that heat treatment at 550 C will not significantly alter the atomic structure of Hap, is in excellent accord with our findings. As shown in Fig. 3(d), however, the XRD patterns of free zinc powders calcined at 1000 °C were distinct from those produced at 550 °C. The findings confirmed the achievement of the desired highly crystalline structure. In Fig. 3(d), the XRD pattern of sample 0ZH2 showed a peak for tricalcium phosphate at 2 = 30.9. (-TCP). Research indicates that calcination at 1000 °C may reduce

the quality of Hap powders. While syn-Q7 modelling predicted that the high crystalline powder would also have a zinc component of 4 at.

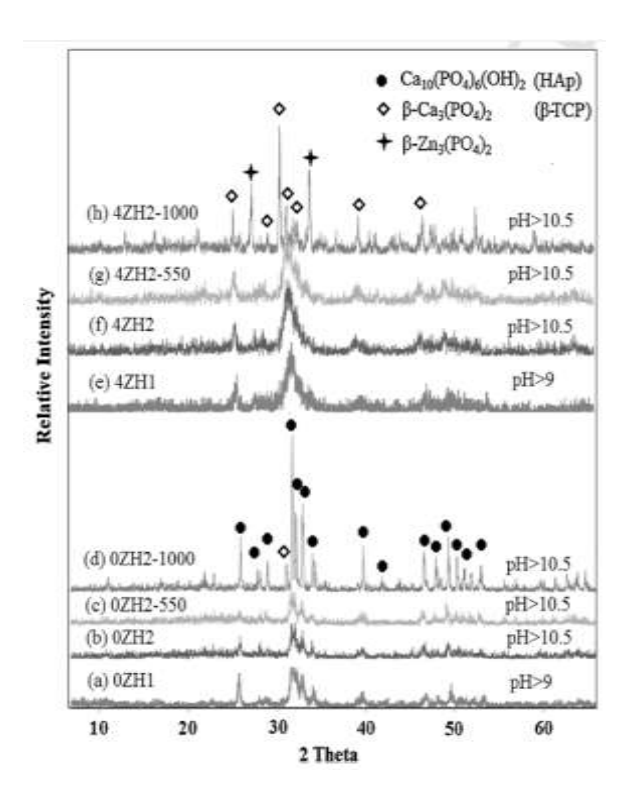


Fig. 3. The effect of pH values and temperature on X-ray diffraction pattern of (a) 0ZH1, (b) 0ZH2, (c) 0ZH2-550, (d) 0ZH2-1000, (e) 4ZH1, (f) 4ZH2, (g) 4ZH2-550 and (h) 4ZH2-1000.

was quite dissimilar to the Hap structure of other lines. The diffraction pattern of 4ZH2-1000 shows that the -TCP peak at 2 = 30.9is more pronounced than in 0ZH2, and that it is complemented by additional peaks relating to another phase. After undergoing a series of calcinations at 1000 C, the Zn2+cations integrated into the Hap structure are thought to have been removed, giving rise to the tri zinc phosphate phase [Zn3(PO4)2].

Internal molecular bonds

Figure 4 displays the FTIR spectra of produced free zinc and integrated Hap at a range of pH levels and temperatures. FTIR spectra of 0ZH1 and 4ZH1 powder samples showed functional vibration bonds of PO43, OH, HPO42, and CO32 at 560-600 cm1 and 956-1031 cm1, 3576 cm1, 875 cm1, and 1423-1565 cm1respectively (Fig. 4(a) and (e)). The universal chemical formula for these clusters is shown in El (1). Carbon dioxide, a prevalent pollutant in the environment, might be dissolved in solution during the precipitation process, integrated into the amorphous complex, and then penetrate into low crystalline Hap. The following reaction (Eq. (3)) [17] dissolves carbon dioxide in the air:

$$CO_{2(g)} + 2OH_{(aq)}{}^{-} \rightarrow \ CO_{3(aq)}{}^{2-} + H_2O_{(1)}$$

Although no entirely new functional groups formed or vanished in the FTIR spectra of the two powder types when the pH was raised (Fig. 4(b) and (f)), the already-present groups underwent minor shifts to other wavenumbers.

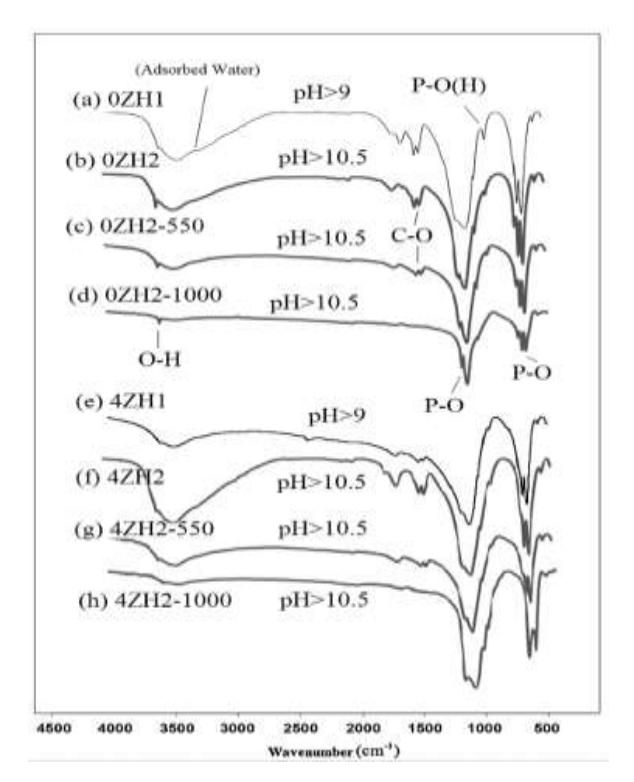


Fig. 4. The effect of pH values and temperature on FTIR spectrum of (a) 0ZH1, (b) 0ZH2, (c) 0ZH2-550, (d) 0ZH2-1000, (e) 4ZH1, (f) 4ZH2, (g) 4ZH2-550 and (h) 4ZH21000.

numerically and qualitatively in terms of heightened intensity. P O bonds in the atomic structure of nap have been reinforced leading to an increasing P O band in FTIR spectra, as seen when comparing the spectra of 0ZH1 and 0ZH2. The P (OH) band in the 0ZH2 spectra was also much weaker compared to that of the 0ZH1 sample. Transmitted bands of P O(H) at 875 cm1 and O H at 3576 cm1 have been reduced by an impact of pH correction, but otherwise the FTIR spectra of powders containing 4 at.% Zn was not noticeably different from the undoped nap. Doping with the zinc contaminate also altered the P O band's characteristics, which, taken along with the XRD data, suggest a reduction in crystallinity. Although the incorporation of CO32 into the atomic structure of Hap is inhibited by the formation of calcium vacancies via the prepa-Q9 ration of zinc doped Hap due to the opposition of electrostatic charges, an increase in pH causes an increase in the incorporation of CO32 into the crystalline of Hap as shown in El (3). This means that the carbonate band in the FTIR spectra of the two produced powders did not shift noticeably while the pH was

changed. Calcination at 500 degrees Celsius narrowed the O H band relative to the 3500 cm1 of adsorbed water. This resulted in the clear manifestation of the O H band immediately next to the functional group in the nap structure. In addition, calcination often results in a faint CO32 band. Adsorbed water was released from samples when Q10 was calcinated at 1000C. Although the C O bands vanished in the FTIR spectra of free zinc and doped in nap (Fig. 4(d) and (h)), calcination had an effect on the integration of carbonate into the atomic structure of nap. After calcination at 1000 C, the FTIR spectra of sample 0ZH showed that it has incorporated key functional group components such PO43 and OH. Regarding alterations in nap's crystallinity, a shoulder has also emerged close to the P OQ11 band. Accordingly, the XRD data and the results of the most recent example show a good agreement, suggesting that the Hap and TCP phases were generated. Although the FTIR of the 4ZH21000 sample was included in both groups, the PO43 group was the only one to get a sample of the 4ZH21000. Consequently, the PO43 ionic group contains a calcium atom and a zinc atom bound together as TCP, also known as tri-zinc phosphate. X-ray diffraction analysis of this sample (Fig. 4(h)) revealed that calcium phosphate and zinc phosphate were the most abundant phases.

Crystallite and particle size

Particle and crystallite size distributions of produced n-hexahydro quinoline (nap) doped and undoped zinc at various pH values were examined.

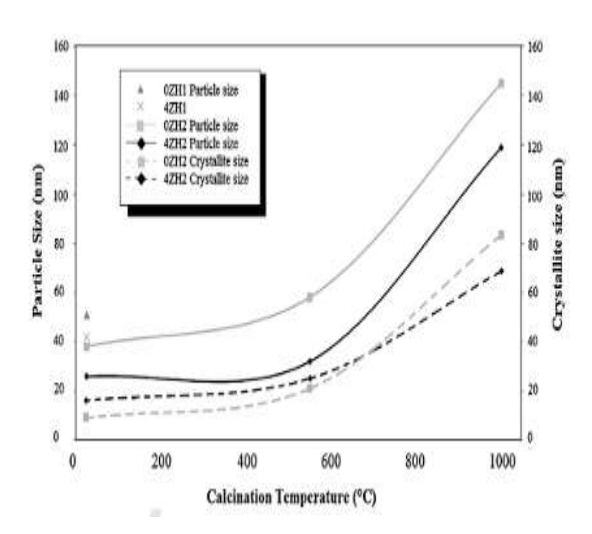
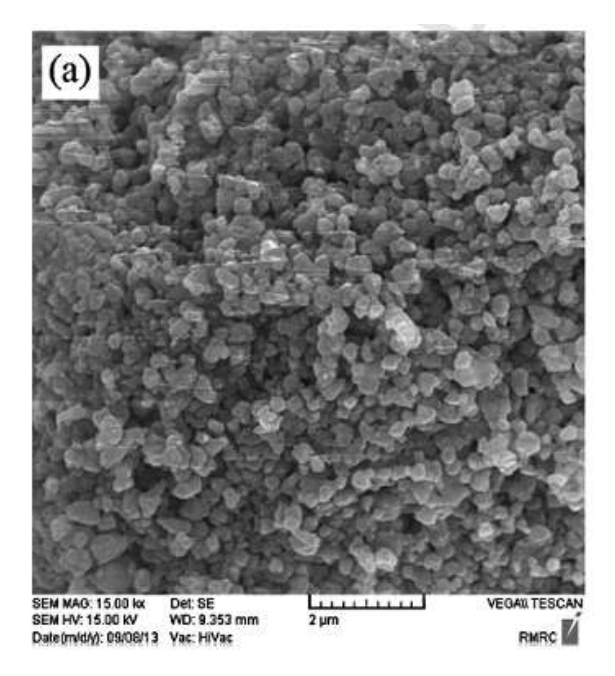


Fig. 5. Average particle size and crystallite size of the synthesized powders at different condition versus calcination temperatures.

temperatures are shown in Fig. 5. The findings indicate that smaller particles develop in both compositions when pH increases, and zinc is doped in. The Scherrer method's calculations for the

materials' nano crystalline nature were verified by the SEM analysis. The findings showed that, when the calcination temperature was raised, the crystallites grew along with the particles. By raising the temperature to 550 degrees Celsius, the crystallite and particles expanded. As compared to 0ZH particles, the nap particles with zinc doping grew by 52%. Since the 550°C XRD and FTIR data demonstrated that the powders' composition and phase were unchanging, the growth of crystallite dependent on the growth of the lattice network, which led to an increase in particle size. The formation of coarser particles with a bigger crystallite size was also seen at a higher Q12 (1000C). calcination temperature Zinc-free powders had an average particle size of 120 14 nm, whereas powders with zinc added had an average particle size of 145 18 nm. As compared to 4ZH particles, which grew by just 280%, 0ZH particles expanded by 350. In the instance of Hap containing Zn2+, heat treatment was observed to induce the crystal to disintegrate to a new composition with smaller particle size than the original Hap. As a result, 4ZH powders with the composition attained a smaller crystallite size than 0ZH powders. Figure 6(a) and (b) are typical SEM images of particles calcined at 1000 °C (b). Particles that are typical of free zinc



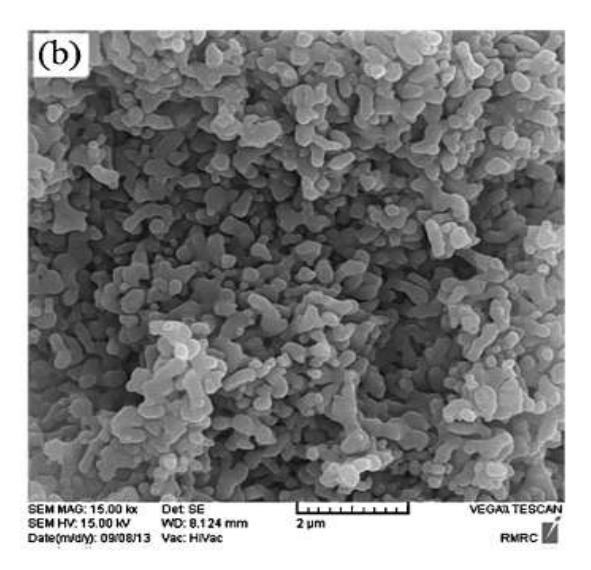


Fig. 6. SEM images of synthesized powders with different composition. (a) Entire and (b) Zn incorporated nap. pH 10.5 and T = 1000°C.

and zinc doped nap have a more consistent size and shape distribution.

Conclusion

Particle size, chemical make-up, and structure of zinc-incorporated Hap were all studied, as were the results of varying pH and calcination. Crystalline single-phase Hap has been precipitated, as shown by XRD and FTIR analysis of both zinc-free and zinc-incorporated powders. A look at the EDS data confirmed the formation of nap. Changing the pH or calcining at 550 degrees Celsius had no effect on the development of the phases, while calcining zinc-free powder at 1000 degrees Celsius led to the crystallisation of Hap containing a trace quantity of -TCP. The zinc cations dissolved in the solution degraded the nap to the simpler compounds TCP and TZP. When the pH was lowered to 10.5, Q14 precipitated with reduced particle size, or with smaller crystallites. According to the SEM analysis, calcination had a greater impact on zinc-doped nap powders than powders without zinc. Particles of both uniform size and irregular shape were seen in the SEM pictures. The findings show that biphasic calcium and zinc phosphate was formed during calcination at 1000C, making this material an excellent candidate for application in controlledrate biodegradation.

References

[1] P. Maughamian, A. Najafi, A. Afshar and J. Javad pour, Adv. Powder Technol., Q15 744–751, (2012).

[2] K. Shitara, H. Murata, K. Watanabe, C. Kojima, Y. Sumida, A. Nakamura, A. Nakahira, I. Tanaka and K. Matsunaga, J. Asian Ceram. Soc., 2, (1) 64–67 (2014).

- [3] S.C. Cox, P. Jamshidi, L.M. Grover and K.K. Mallick, Mater. Sci. Eng. C, 35, 106–114 (2014).
 [4] D. Xie, I.D. Chung, G. Wang, D. Feng and J. Mays, Eur. Polyp. J., 40, 1723–1731 (2004).
- [5] K. Ishikawa, Y. Miyamoto, T. Yuasa, A. Ito, M. Nagayama and K. Suzuki, Biomaterials, 23, (2) 423–428 (2002).
- [6] P. Bhattacharjee, H. Begam, A. Chanda and S.K. Nandi, J. Asian Ceram. Soc., 2, (1) 64–67 (2014).
- [7] R.M.B. Faria, D.V. Cesar and V.M.M. Salim, Catalo. Today, 133, 168–173 (2008).
- [8] I. Uysal, F. Sever can and Z. Evis, Ceram. Int., 39, (7) 7727–7733 (2013).
- [9] E. Fujii, M. Ohkubo, K. Tsuru, S. Hayakawa, A. Osaka, K. Kawabata, C. Bonhomme and F. Bonneau, Acta Biomatter., 2, (1) 69–74 (2006).
- [10] K. Kawabata, T. Yamamoto and A. Kitada, J. Phys. B, 406, 890–894 (2011).
- [11] A. Reaching and M.M. Kashani Motlagh, Int. J. Phys. Sci., 7, (20) 2768–2774 (2012).
- [12] S.V. Droshky, Acta Biomatter., 6, 4457–4475 (2010).
- [13] A. Gowalia, A. Behnam Hadera, M. Deliria and A. Moschiferous, Sci. Iran. F, 18, (6) 1614–1622 (2011).
- [14] I. Cacciotti and A. Bianco, Ceram. Int., 37, (1) 127–137 (2011).
- [15] B.B. Cullity and B. Dennis, Directions of Diffracted Beams, Elements of X-rayQ16 Diffraction, 3rd ed., Addison-Wesley (2001).
- [16] F. Miyaji, Y. Kono, and Y. Suyama, Mater. Res. Bull., 40, 209–220 (2005). [17] S. Kangri, K. Jan Pradit, K. Bupa, S. Techawongstien and S. Chant, Chem. Eng. J., 215–216, 522–532 (2013).